



Article

Exposure to Benzo(a)pyrene Enhances Acetaminophen-Induced Liver Injury in Mice at Non-Hepatotoxic Doses

Yina Montero-Pérez  and Jesus Olivero-Verbel * 

Environmental and Computational Chemistry Group, School of Pharmaceutical Sciences, Zaragocilla Campus, University of Cartagena, Cartagena 130014, Colombia; yina.montero@gmail.com

* Correspondence: joliverov@unicartagena.edu.co

Abstract: Acetaminophen (APAP) is a widely used analgesic, especially for children. Its primary mechanism involves inhibiting cyclooxygenase enzymes and activating the endocannabinoid and TRPV1 systems. Though its toxicity is low, it can harm the liver in a dose-dependent manner. Low APAP doses can also increase pollutant-induced liver damage. Little is known about interactions between APAP and benzo[a]pyrene (B[a]P). This study aimed to assess if co-exposure to non-hepatotoxic doses of B[a]P and APAP causes liver injury in mice, exploring the underlying mechanisms. Female ICR mice received 50 mg/kg B[a]P or a vehicle for three days, followed by 200 mg/kg APAP or a vehicle. Liver injury was assessed through histopathological examination, serum transaminase activity, and gene expression analysis. In the B[a]P/APAP group, several histology changes were observed, including ballooning injury, steatosis, necrosis, inflammation, and apoptosis. Transaminase levels correlated with histopathological scores, and there was an increase in hepatic cytochrome P450 family 1 subfamily a member 1 (*Cyp1a1*) mRNA levels and a decrease in aryl hydrocarbon receptor (*Ahr*), cytochrome P450 family 2 subfamily e polypeptide 1 (*Cyp2e1*), superoxide dismutase 1 (*Sod1*), peroxisome proliferator activated receptor gamma (*Ppar-γ*), and caspase 3 (*Casp3*). This suggests that prior exposure to B[a]P makes mice more susceptible to APAP-induced liver injury, involving changes in gene expression related to metabolism, redox balance, and cell proliferation. Therefore, using therapeutic APAP doses after exposure to B[a]P could lead to liver injury.

Keywords: acetaminophen; benzo[a]pyrene; hepatotoxicity; toxicological interaction; oxidative stress



Citation: Montero-Pérez, Y.; Olivero-Verbel, J. Exposure to Benzo(a)pyrene Enhances Acetaminophen-Induced Liver Injury in Mice at Non-Hepatotoxic Doses. *Sci. Pharm.* **2024**, *92*, 30. <https://doi.org/10.3390/scipharm92020030>

Academic Editor: Valentina Onnis

Received: 29 February 2024

Revised: 6 May 2024

Accepted: 10 May 2024

Published: 3 June 2024



Copyright: © 2024 by the authors. Licensee MDPI, Basel, Switzerland. This article is an open access article distributed under the terms and conditions of the Creative Commons Attribution (CC BY) license (<https://creativecommons.org/licenses/by/4.0/>).

1. Introduction

Acetaminophen (APAP) is one of the most popular and widely used analgesic and antipyretic drugs globally [1,2], and it is included in the WHO model list of essential medicines [3]. Although this chemical is safe for most individuals, there is a risk of developing drug-induced liver injury (DILI) in some patients with pre-existing pathological conditions such as liver damage [4], malnutrition [5,6], co-medication [7], age [8], genetics [9], or tobacco consumption [10], among others [1].

Once ingested, most APAP is excreted in bile and urine after combination with glucuronide and sulfate cofactors, and a fraction of APAP (5–10%) is metabolized to N-acetyl-p-benzoquinone imine (NAPQI) [1], which is detoxified through conjugation with glutathione [11,12]. This last reaction can lead to cellular oxidative stress by glutathione depletion, reducing the ability of glutathione transferase to metabolize hydrogen peroxide [2,12]. During an APAP overdose, large amounts of NAPQI are produced, depleting liver glutathione and causing liver injury [11,12]. Acetaminophen overdose is the most frequent cause of acute liver failure (ALF) of any etiology in the United States (46%), and in Great Britain and Europe (40–70%) [13], APAP-induced liver damage represents the second most common cause of liver transplantation worldwide [14], being responsible for about 500 deaths per annum in the United States (U.S.) alone [15] and 150 to 200 deaths annually in England and Wales [16].

The molecular mechanisms underlying acetaminophen-induced liver damage have been extensively studied [11,17,18]. One of the primary molecular pathways implicated in the progression of APAP-induced liver injury involves the induction of oxidative stress, triggered by the production of the reactive metabolite NAPQI through acetaminophen metabolism via cytochrome P450 (Cyp450), primarily CYP2E1 [19]. NAPQI, capable of forming adducts through its interaction with cysteine groups of proteins [11,17,18], leads to the formation of mitochondrial permeability transition pores, resulting in disruptions in calcium homeostasis, uncoupling of oxidative phosphorylation, release of intramitochondrial ions and metabolic intermediates, mitochondrial inflammation, decreased ATP synthesis, and ultimately, hepatocyte viability loss [17].

In addition to the tissue damage induced by oxidative stress events resulting from APAP metabolites, several studies have also implicated APAP in potential genotoxic and carcinogenic effects. This is attributed to the formation of the quinone imine (NAPQI), which can chemically interact with DNA through a 1,4-Michael addition mechanism, following depletion of glutathione (GSH) [20].

The antioxidant defense mechanisms against APAP-induced oxidative stress processes have been extensively described [11,21,22]. The formation of NAPQI-protein adducts in the mitochondrial respiratory chain (MRC) triggers the release of electrons to oxygen, thereby promoting the production of superoxide, which is then catalyzed into hydrogen peroxide and oxygen by superoxide dismutase (SOD), leading to oxidative/nitrosative stress [11,22,23]. Hydrogen peroxide is either eliminated by catalase (CAT) or reacts with GSH. Consequently, when GSH levels decrease, and antioxidant activity is inhibited, reactive oxygen species combine with nitric oxide (NO) to form peroxynitrite, resulting in the formation of nitrotyrosine adducts that affect the function of intracellular proteins [11].

One of the exogenous factors recently studied concerning variations in drug effects and toxicity is related to individuals' exposome. This is because it can alter drug metabolism, change the bioavailability or excretion of the drug, or interfere with drug action and targets [24].

The exacerbation of APAP-induced liver injury has been demonstrated by studies involving pre-exposure or co-exposure of biomodels to various pollutants, including ozone [25], fenbendazole [26], and roxithromycin [27], among others [28,29]. Within the reported toxicological interaction mechanisms from these investigations, several have been identified: increased oxidative stress, evidenced by significant expression of oxidative stress-responsive genes such as metallothionein-1 (*Mt-1*), heme oxygenase-1 (*Hmox-1*), and glutamate-cysteine ligase (*Gclc*) in the liver, and reduced cellular regeneration mechanisms due to overexpression of *P21* [25]; depletion of tissue GSH levels due to the formation of conjugates [26]; and induction of oxidative stress through metabolic changes in each xenobiotic by inhibiting cytochrome P450 2D6 (CYP2D6) activity and increasing cytochrome P450 2E1 (CYP2E1) expression, leading to slower APAP elimination [27]. These findings raise significant concerns, especially considering the multitude of environmental pollutants that are part of our daily exposome, which may be involved in the depletion of endogenous antioxidants. This is particularly worrisome as their mechanisms of action may coincide with that of APAP. Among these chemicals are the polycyclic aromatic hydrocarbons (PAHs), in particular benzo[a]pyrene (B[a]P), known for their capacity to induce oxidative stress [30–32]. Benzo[a]pyrene is considered a high-priority substance of concern for human exposure (8th/275), according to the Agency for Toxic Substances and Disease Registry [33]. B[a]P is generated through pyrolytic processes, particularly the incomplete combustion of organic materials during industrial and other human activities [34]. This xenobiotic has been repeatedly found in the air, surface water, soil, and sediments [35–37]. Human exposure to B[a]P is common [35], considering its sources of contamination in the environment, which include industrial and automobile emissions, hazardous waste sites, cigarette smoke, biomass burning, municipal incinerators, volcanic eruptions, home heating, and the consumption of charcoal-broiled and smoked foods [34,38].

This PAH has been categorized by the International Agency for Research on Cancer (IARC) as a human group 1 carcinogen because of its mutagenic and carcinogenic effects in animal models and its association with the development of several types of human cancer, including lung, breast, and liver [38,39]. In addition to sufficient evidence of carcinogenicity in humans, the neurotoxicity, epigenotoxicity, alteration of various metabolic pathways, and reproductive toxicity of B[a]P have been demonstrated experimentally [31,35,38–42]. The molecular mechanisms associated with B[a]P toxicity involve the creation of stable and depurinating DNA adducts, repetitive redox cycling that generates reactive oxygen species (ROS), radical-cation mechanism, mechanism via formation of ortho-quinone, and interaction with the aryl hydrocarbon (AhR) receptor, among others [39,43].

Due to its lipophilicity, B[a]P is readily absorbed through biological membranes and undergoes bioactivation to reactive metabolites mediated by enzymes from the Cytochrome P450 (CYP) superfamily, including cytochrome P450 1A1 (CYP1A1), cytochrome P450 1A2 (CYP1A2), and cytochrome P450 1B1 (CYP1B1), resulting in the production of ROS and metabolites such as phenol forms, epoxides, dihydrodiols, dihydrodiol epoxides, and anti-7,8-dihydroxy-9,10-epoxy-7,8,9,10-tetrahydro-B[a]P [30,32,35,38,44,45]. It has been demonstrated that the production of B[a]P-7,8-epoxide, mediated by CYP1A1, and its subsequent transformation to B[a]P-trans-7,8-dihydrodiol (B[a]P-7,8-DHD) in the presence of epoxide hydrolase represent dangerous reactions, as B[a]P-7,8-DHD is converted to the carcinogenic metabolite 7 β ,8 α -dihydroxy-9 α ,10 α -epoxy-7,8,9,10-tetrahydrobenzo[a]pyrene (BPDE), which creates DNA adducts, causing mutations and malignant transformations [35,46]. Additionally, B[a]P-trans-7,8-dihydrodiol can undergo oxidation processes mediated by aldo-keto reductases (AKR) [47], resulting in the production of benzo[a]pyrene-7,8-dione (B[a]P-7,8-dione), which is an ortho-quinone metabolite of B[a]P. This metabolite can undergo a 1,4- or 1,6-Michael addition with glutathione (GSH) and N-acetyl-L-cysteine (NAC) [48], which has been established as the antidote to APAP poisoning and overdose since 1974 due to its ability to increase hepatic levels of glutathione, facilitating the scavenging of reactive metabolites and reactive oxygen species [49].

The cellular antioxidant system, including key enzymes such as superoxide dismutase (SOD), glutathione peroxidase (GPx), catalase (CAT), and non-enzymatic components like glutathione, plays a crucial role in eliminating or regulating the elevated levels of ROS produced in the body [30]. Despite this, some studies have demonstrated disturbances in antioxidant responses in the liver, lungs, kidneys, stomach, and brain induced by acute B[a]P treatment in a murine model [30,32].

APAP and B[a]P hepatotoxicity is associated with alterations in the activity of metabolic enzymes, including members of the Cytochrome P450 family [17,19,31,43–45]; the generation of reactive byproducts, leading to the depletion of endogenous antioxidants produced during their metabolism [17,20,26,30,32]; as well as the activation or inactivation of transcription factors through their interaction with specific ligands. These factors, in turn, regulate the expression of genes involved in the metabolism and toxicity of these xenobiotics [50–52].

Despite the evident co-exposure to acetaminophen and B[a]P, especially in individuals who smoke cigarettes, are exposed to automobile emissions, and consume food contaminated with B[a]P, there is insufficient information regarding the effects of pre-exposure to B[a]P on non-hepatotoxic doses of acetaminophen-induced liver damage. Therefore, the objective of this research was to evaluate whether acute co-exposure to non-hepatotoxic doses of B[a]P and APAP could induce liver injury in mice and to explore the cellular and molecular mechanisms involved.

2. Results

2.1. Body Weight and Liver-to-Body Ratio

Mice body weight did not show significant alterations following various treatments, including sesame oil (vehicle for B[a]P) and saline solution (vehicle for APAP), APAP alone, B[a]P alone, or B[a]P combined with APAP (Figure S1). However, a noteworthy increase

($p < 0.05$) in the liver-to-body weight ratio was observed in the group of mice treated with B[a]P and B[a]P combined with APAP compared to the control. No significant difference was observed between the control group and the group treated with APAP alone (Figure 1).

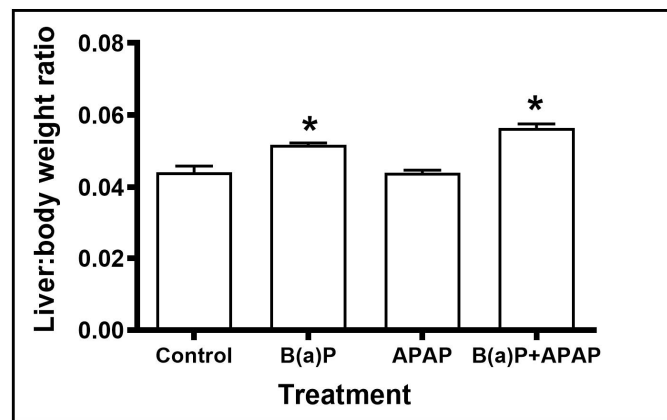


Figure 1. Effects of B[a]P/APAP co-exposure on the relative liver weight for the different experimental groups. The mice group exposed to B[a]P and B[a]P + APAP exhibited a significant increase in the liver-to-body weight ratio compared to the control group. Control, non-exposure group ($n = 5$); B(a)P, animals treated with B[a]P ($n = 7$); APAP, mice treated with APAP ($n = 6$); B(a)P + APAP, animals treated with B[a]P and APAP ($n = 12$). Data are expressed as mean \pm SEM. * indicates significantly different control group. The level of significance was set at $p < 0.05$.

2.2. Serum Transaminase Activity

Alanine aminotransferase (ALT) and Aspartate aminotransferase (AST) activities were investigated as markers of hepatocellular injury in circulating blood. A significant increase ($p < 0.05$) in the activity of these transaminases was detected in the serum of mice in the group that received the co-treatment of B[a]P and APAP compared to the control group (Figure 2).

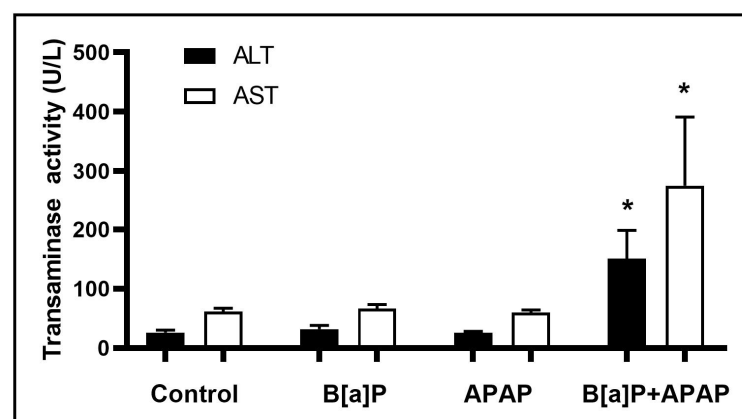


Figure 2. Serum ALT and AST levels in different treatment groups. Serum ALT activity was significantly elevated in B[a]P + APAP-treated mice. Control, non-exposure group ($n = 5$); B(a)P, animals treated with B[a]P ($n = 7$); APAP, mice treated with APAP ($n = 6$); B(a)P + APAP, animals treated with B[a]P and APAP ($n = 12$). Each bar represents the mean \pm SEM. * indicates significantly different control group. The level of significance was set at $p < 0.05$.

2.3. Relative Gene Expression

The results of the gene expression profile for all experimental groups are shown in Figures 3 and S2 and Table S2. B[a]P/APAP treatment caused changes in the relative expression of various genes coding for proteins involved in different biochemical processes. B[a]P/APAP co-exposure led to a significant increase in the expression of *Cyp1a1*

(Cytochrome P450 Family 1 Subfamily A Member 1), which is a gene encoding one of the enzymes responsible for the metabolism of xenobiotics, including B[a]P, and a decrease in the expression of the genes *Ahr* (Aryl Hydrocarbon Receptor), *Cyp2e1* (Cytochrome P450 Family 2 Subfamily E Member 1), *Sod1* (Superoxide Dismutase 1), *Ppar-γ* (Peroxisome Proliferator-Activated Receptor Gamma), *Casp3* (Caspase 3), and *Trp53* (Transformation-related Protein 53). These results suggest that B[a]P/APAP co-exposure promotes alterations in *Ahr* activation, oxidative stress, lipid and xenobiotics metabolism, and apoptosis pathways.

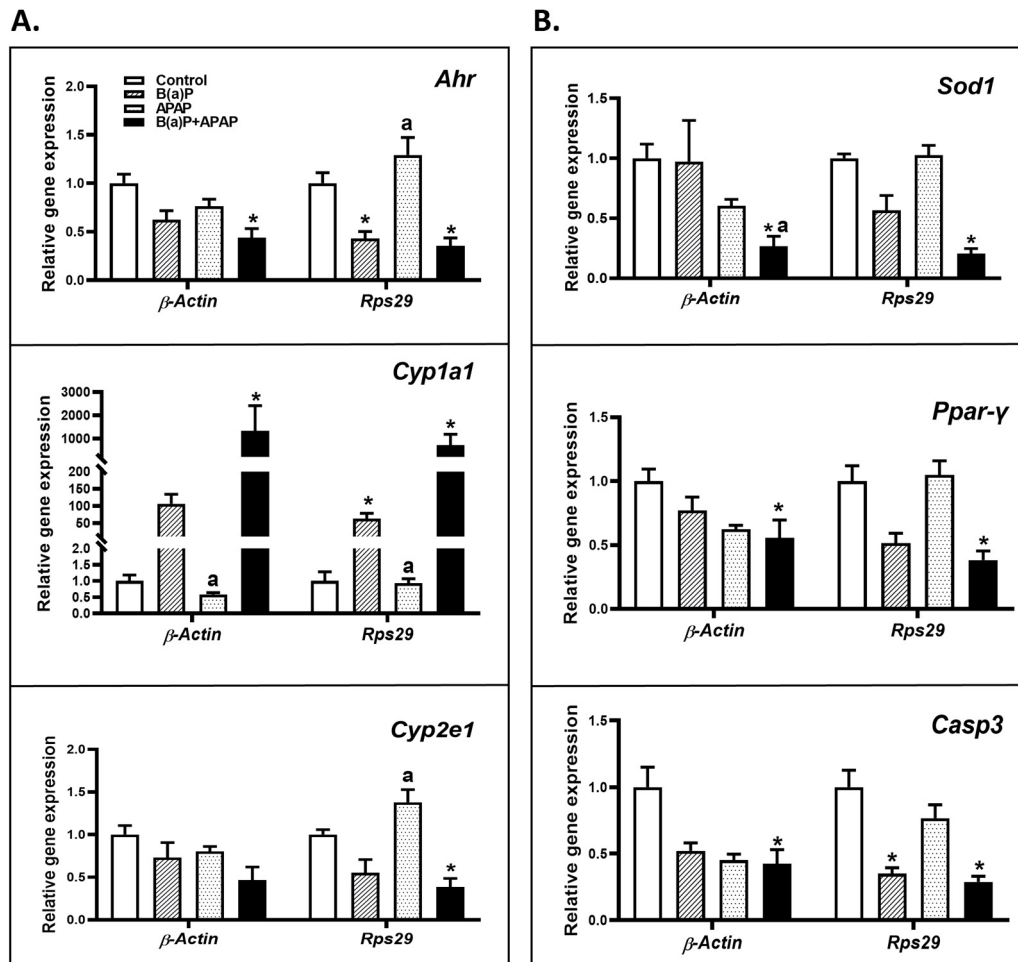


Figure 3. Effects of B[a]P/APAP co-exposure on the mRNA levels of target genes in the liver of ICR mice. (A). Genes involved in xenobiotic metabolism (B). Genes related to oxidative stress and apoptosis. Expression was normalized against β -Actin and *Rps29* (housekeeping genes). Control, non-exposure group ($n = 5$); B(a)P, animals treated with B[a]P ($n = 7$); APAP, mice treated with APAP ($n = 6$); B(a)P + APAP, animals treated with B[a]P and APAP ($n = 12$). Data are expressed as mean \pm SEM. * indicates significantly different from control group; a indicates significantly different from B[a]P group. The level of significance was set at $p < 0.05$.

2.4. Pathological Examination

Examination of liver tissue showed very few or no histological alterations in the liver of the control, APAP-, and B[a]P-treated mice. B[a]P/APAP treatment caused several hepatic changes found in the B[a]P/APAP group, including ballooning injury, steatosis, necrosis accompanied by lobular and portal inflammation, and apoptosis (Figure 4). The sum of hepatic histopathological scoring was significantly increased ($p < 0.05$) in mice treated with B[a]P/APAP (Table 1; Figure S3A). Additionally, a good correlation was found between transaminase values and the histopathological scores obtained (Figure S3B).

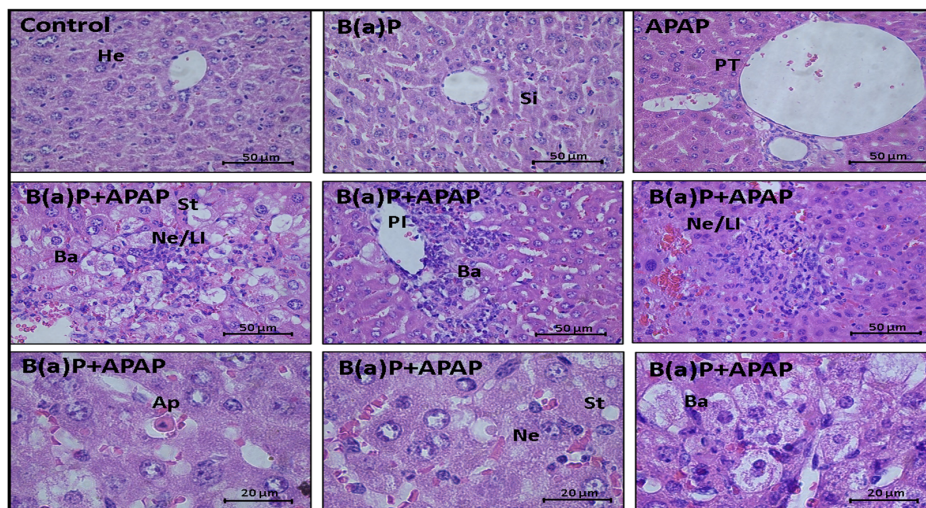


Figure 4. Effects of B[a]P/APAP on hepatic morphology of ICR mice. Light photomicrographs of liver sections from the control group, mice exposed to APAP alone, B[a]P alone, or a combination of B[a]P and APAP. Hematoxylin and eosin staining (H&E) (40× and 100×). He, hepatocytes with normal architecture; Si, sinusoids; PT, portal triad (portal vein, hepatic artery, and bile duct); Ba, ballooning injury; St, steatosis; Ne, necrosis; LI, lobular inflammation; PI, portal inflammation; Ap, apoptosis.

Table 1. Scoring of hepatic histopathological examinations from different groups of mice exposed to APAP, B[a]P, and APAP + B[a]P.

Treatment	Severity	Frequency of Histopathological Parameters					Σ Frequency of Total Histopathological Finding per Severity	Mean of Total Hepatic Histopathological Scoring
		Ballooning	Steatosis	Portal Inflammation	Lobular Inflammation	Necrosis		
Control <i>n</i> = 5	0	5	5	5	5	5	0	0.00
	1	0	0	0	0	0	0	
	2	0	0	0	0	0	0	
	3	0	0	0	0	0	0	
APAP <i>n</i> = 6	0	6	6	6	5	6	0	0.17
	1	0	0	0	1	0	1	
	2	0	0	0	0	0	0	
	3	0	0	0	0	0	0	
B(a)P <i>n</i> = 7	0	7	7	7	7	6	0	0.14
	1	0	0	0	0	1	1	
	2	0	0	0	0	0	0	
	3	0	0	0	0	0	0	
B(a)P + APAP <i>n</i> = 12	0	5	5	8	4	2	0	5.17
	1	2	4	2	5	4	17	
	2	2	3	1	3	3	24	
	3	3	0	1	0	3	21	

In severity, 0: absent or rare, 1: mild, 2: moderate, 3: marked. The internal numbers in each histopathological parameter correspond to the number of mice for each degree of severity (frequency). Total histopathological finding per severity was calculated as the sum of the product of the level of severity × number of mice with the corresponding level of severity for each histopathological parameter.

3. Discussion

The findings reported here indicate that previous exposure to polynuclear aromatic hydrocarbons can potentiate the hepatotoxicity of APAP, evidenced by changes in gene expression, increased transaminase levels, and histopathological markers of tissue damage.

The liver plays a crucial role in maintaining various physiological processes related to the immune and endocrine systems as well as in metabolism and the detoxification

of xenobiotics, including polycyclic aromatic compounds and drugs [53]. In this study, both B[a]P alone and B[a]P + APAP treatments induced an increase in the liver-to-body weight ratio. This increase in the relative weight of the liver, as observed in previous studies involving male and female F-344 rats exposed to B[a]P [54], may be indicative of an adaptive response within the liver aimed at maintaining the organism's homeostasis. Such adaptation could involve alterations in enzymatic activity [55], as demonstrated in this study (Figure 3A).

The molecular pathogenesis of APAP and B[a]P has been extensively described [11, 18,39,43]. Both xenobiotics undergo bioactivation processes mediated by enzymes from the CYP450 superfamily, including cytochrome P450 1A1 (CYP1A1), cytochrome P450 1A2 (CYP1A2), and cytochrome P450 1B1 (CYP1B1), involved in B[a]P metabolism [56], and cytochrome P450 2E1 (CYP2E1), cytochrome P450 1A2 (CYP1A2), and cytochrome P450 3A4 (CYP3A4), responsible for APAP bioactivation [57], resulting in the generation of ROS and B[a]P derivatives such as phenol forms, epoxides, dihydrodiols, dihydrodiol epoxides, and anti-7,8-dihydroxy-9,10-epoxy-7,8,9,10-tetrahydro-B[a]P [30,32,35,38,44,45] as well as NAPQI, derived from APAP metabolism [11,14]. The toxicological significance of these byproducts lies in their ability to form protein adducts, leading to the alteration of various cellular functions. For instance, NAPQI induces alterations in mitochondrial membrane permeability, disruptions in calcium homeostasis, alterations in oxidative phosphorylation, release of intramitochondrial ions and metabolic intermediates, oxidative stress, decreased ATP synthesis, and ultimately, loss of hepatocyte viability [11,17,18]. Moreover, NAPQI has been shown to chemically interact with DNA through a 1,4-Michael addition mechanism, following depletion of glutathione (GSH) [20]. Some B[a]P byproducts, such as tetrahydrobenzo[a]pyrene (BPDE), can also form DNA adducts causing mutations and malignant transformations [35,46], while benzo[a]pyrene-7,8-dione (B[a]P-7,8-dione) can undergo a 1,4- or 1,6-Michael addition with glutathione (GSH) and N-acetyl-L-cysteine (NAC) [48], which is used as the antidote to APAP poisoning and overdose [49]. At low doses, the individual effects of these chemicals are negligible due to the activation of cellular antioxidant response mechanisms. However, in combination, the toxicological interaction of these xenobiotics could contribute to the depletion of tissue GSH levels due to the formation of conjugates with B[a]P-7,8-dione and NAPQI, metabolic changes in each xenobiotic by alteration in the expression of genes encoding enzymes of the Cytochrome P450 superfamily, as well as cell death [32]. This has been demonstrated in several studies of toxicological interaction between APAP and other xenobiotics such as ozone [25], fenbendazole [26], and roxithromycin [27], among others [28,29], and between B[a]P and other chemicals such as silica nanoparticles [58] and lead [59]. These interaction mechanisms could explain the increase in transaminase levels (Figure 2); the downregulation of gene expression for *Ahr*, *Cyp2e1*, *Sod1*, *Ppar-γ*, *Casp3*, and *Trp53* (Figure 3); as well as the liver tissue damage found in the group of mice treated with B[a]P + APAP (Figure 4).

The treatment with B[a]P induced a pronounced increase of *Cyp1a1* gene expression, which was exacerbated by APAP (Figure 3A). This gene encodes a member of the Cytochrome P450 superfamily of enzymes involved in both B[a]P detoxification and metabolic activation. The latter process results in DNA adduct formation and reactive oxygen species (ROS) production [60]. It is well established that B[a]P binds to the aryl hydrocarbon receptor (Ahr), a ligand-dependent transcription factor, and induces the transcription of genes involved in various pathways, including xenobiotic and lipid metabolism, and immune responses, such as *Cyp1a1* (Cytochrome P450, family 1, subfamily a, polypeptide 1), *Cyp1b1* (Cytochrome P450, family 1, subfamily b, polypeptide 1), *Fabp5* (fatty acid binding protein 5), *Ugdh* (UDP-glucose dehydrogenase), *Car3* (Carbonic anhydrase 3), *Nqo1* (NAD(P)H dehydrogenase, quinone 1), *Myc* (Myelocytomatosis oncogene), and *Mt1* (Metallothionein 1), among others [61]. Due to the involvement of the AHR protein in various biological processes, cells have developed different mechanisms to prevent excessive signaling. One of these mechanisms involves the overexpression of phase I and II enzymes of xenobiotic metabolism, facilitating their removal through ATP-dependent membrane transporters [62].

CYP1A1 exhibits a high capacity for AHR-mediated metabolism and activation of B[a]P [60], resulting in the generation of B[a]P 7,8-epoxide; B[a]P 7,8 diols; B[a]P 7,8-dihydrodiol-9,10-epoxide (BPDE); and reactive oxygen species (ROS) as by-products of these reactions [30]. In this study, exposure to B[a]P/APAP resulted in a decrease in *Ahr* gene expression compared to the control group (Figure 3A), likely due to negative feedback induced by the degradation of its ligand B[a]P through CYP1A1. This negative feedback mechanism serves to regulate *Ahr* signaling and prevent adverse effects [63].

In addition to its role in B[a]P activation, detoxification, and ROS release through metabolic reactions [30], *Cyp1a1* expression also appears to be involved in the regulation of other Cytochrome P450 enzymes [64]. In this study, *Cyp1a1* was overexpressed in mice treated with B[a]P and those exposed to B[a]P/APAP. However, *Cyp2e1*, which encodes one of the key enzymes involved in metabolizing APAP to its toxic metabolite, was downregulated (Figure 3A). This observation may be attributed to a potential repression of *Cyp2e1* expression by the overexpression of *Cyp1a1* induced by reactive oxygen species produced during its metabolic activity. This inference is supported by a previous study demonstrating the downregulation of the *CYP2E1* gene following exogenous H₂O₂ addition and glutathione depletion mediated by benzo[a]pyrene treatment [65,66].

The conversion of paracetamol to NAPQI, its primary reactive metabolite, is catalyzed by various proteins of the Cytochrome P450 superfamily, predominantly by CYP2E1. However, other isoforms, including CYP1A2 and CYP3A4, also contribute to the bioactivation processes of APAP, as observed by several authors [67–69]. Lee and coworkers demonstrated that other P450 enzymes such as CYP1A2 may be responsible for the toxicity in *Cyp2e1* knockout mice at high doses of APAP (600 mg/kg) [70]. Therefore, the metabolic activation of APAP in the co-exposed group could be promoted by an upregulation of *Cyp1a2* following prior exposure to B(a)P, considering that the expression of *CYP1a2* can be induced by polycyclic aromatic hydrocarbons [71].

The metabolism of APAP leads to the production of N-acetyl-p-benzoquinone imine (NAPQI), a reactive metabolite detoxified by conjugation with glutathione [2,11,14]. As this antioxidant molecule is depleted by APAP, the reactive oxygen species (ROS) production induced by the metabolism of B[a]P deepens the antioxidant arsenal in the cell. Together with the accumulation of NAPQI at low doses of APAP, extensive cell damage occurs, explaining features such as necrosis, apoptosis, inflammation, hemorrhage, and congestion of the liver parenchyma [1,11,72], causing increased levels of aminotransferases [15].

Oxidative stress is largely regulated by the antioxidant enzyme system, including SOD, CAT, GPx, peroxiredoxin (Prx), and glutathione reductase (GSR), among others. Therefore, the loss of expression of these enzymes could be used as biomarkers of oxidative stress [73]. In this study, a downregulation in the expression of genes encoding oxidative stress-scavenging enzymes such as *Sod1* (Figure 3B) and *Hmox1* (Figure S2) was evidenced, suggesting disturbances in the antioxidant system due to the overproduction of epoxides and other B[a]P byproducts [30,32]. It is also known that there are regulatory sequences in the promoter region of the *Sod1* gene that correspond to binding sites for various transcription factors such as AhR, Nrf2, and NF-κB, among others [74]. Thus, the downregulation of *Sod1* could also be associated with the decreased expression of AhR observed in B[a]P/APAP-treated mice, favoring an oxidative cellular environment.

In addition to the molecular alterations implicated in xenobiotic metabolism and the disruption of the antioxidant system resulting from the co-exposure to B[a]P/APAP, an aberration in lipid metabolism was evidenced through the analysis of *Ppar-γ* gene expression, a member of the peroxisome proliferator-activated receptor family. PPAR-γ plays a crucial role in reducing hepatic lipotoxicity and ameliorating steatosis [75] by regulating lipid and glucose metabolism, enhancing glycogen synthesis, and improving mitochondrial function and fat mobilization from muscle/liver tissues [76]. Previous studies have demonstrated that B[a]P can reduce mRNA expression of *Pparγ* in mice, leading to dyslipidemia and abnormal glucose metabolism [77]. Consistent with these findings, in the current study, *Ppar-γ* was downregulated in B[a]P-treated mice, resulting in

alterations in liver morphology, including hepatic steatosis [78] (Figure 4). These metabolic changes could render the liver more susceptible to injury induced by APAP, as indicated by numerous studies involving cell lines, mouse models, and human populations [79–81].

PPAR- γ has been reported to play a role in cancer, acting either as a promoter or a suppressor in tumor cell growth. Its function depends on the signaling pathways activated in the cellular microenvironment through interaction with various ligands [76,82]. Molecular mechanisms involved in its role as an antineoplastic regulator are based on the inhibition of cell proliferation, induction of apoptosis, and terminal differentiation [83,84]. The findings in this study suggest that the downregulation of *Casp3* (Figure 3B) in the B[a]P/APAP group might be mediated by reduced Ppar- γ activity, as demonstrated in mutant mice with follicular thyroid carcinoma (TR $\beta^{PV/PV}$) [85].

The alterations in gene expression observed in the B[a]P/APAP group resulted in hepatic changes including ballooning injury, steatosis, and necrosis accompanied by lobular and portal inflammation (Figure 4). This suggests that prior exposure to B[a]P can elevate the risk of APAP hepatotoxicity even at non-toxic doses, possibly due to the depletion of enzymatic and non-enzymatic endogenous antioxidants that counteract the adverse effects of free radicals produced during benzo(a)pyrene metabolism [30,32]. Additionally, there is a super-production of toxic APAP metabolites through the activation of CyP450 enzymes [52], as evidenced by changes in the expression of genes involved in xenobiotic metabolism, the antioxidant system, lipid metabolism, and the regulation of cell proliferation, such as *Cyp1a1*, *Cyp2e1*, *Sod1*, *Ppar- γ* , and *Casp3*. Consequently, liver tissue damage typical of acetaminophen toxicity is induced, characterized by alterations in liver morphology including vacuolization of centrilobular hepatocytes, steatosis, and necrosis, accompanied by inflammation [72]. The manifestation of liver injury is reflected in the release of high concentrations of liver transaminases detected in the serum (Figure 5). Our results demonstrate a significant association between transaminase levels (ALT and AST) and hepatic histopathological scoring ($p < 0.0001$), with positive correlations ($r = 0.77$ and 0.71 , respectively) (Figure S3).

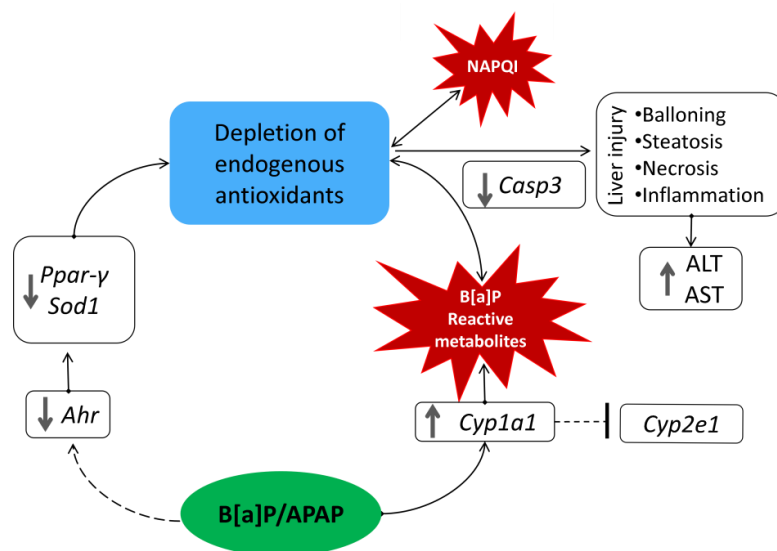


Figure 5. Molecular mechanisms involved in the potentiation of acetaminophen hepatotoxicity by B[a]P. The overexpression of *Cyp1a1* induced by B[a]P leads to the downregulation of *Cyp2e1* and excessive production of reactive metabolites of B[a]P. This, along with the under-expression of the *Sod1* and *Ppar- γ* genes, induces a dysregulation of the redox balance in liver tissue due to the depletion of antioxidants and the downregulation of apoptotic signals via *Casp3*. Thus, exposure to non-hepatotoxic doses of APAP results in the production of NAPQI (possibly mediated by CYP1A2), causing ballooning, steatosis, necrosis, and inflammation as well as the release of elevated levels of serum transaminases such as ALT and AST because of liver injury.

4. Materials and Methods

4.1. Laboratory Animals

Pathogen-free ICR-CD1 female mice (6 weeks old, 18–20 g), obtained from the National Institute of Health (Colombia), were included. The mice were housed in a controlled environment, maintaining a temperature of 25 ± 2 °C, relative humidity of 70–85%, and a 12 h light/dark cycle and were provided with free access to standard rodent food (Laboratory Rodent Diet 5001, St. Louis, MO, USA) and water. Before the commencement of experiments, the mice underwent a 2-week acclimatization period. All procedures were conducted in accordance with the recommendations of the European Union regarding animal experimentation (Directive of the European Council 2010/63/EU) and were approved by the Ethics Committee on Scientific Research at the University of Cartagena (Minute No. 106 of 15 March 2018).

4.2. Experimental Design

Thirty ICR female mice were randomly distributed using a blind method into four groups as follows: group I, the non-exposure group ($n = 5$); group II, animals treated with B[a]P (Sigma-Aldrich, St. Louis, MO, USA) ($n = 7$); group III, mice treated with APAP (Sigma-Aldrich, St. Louis, USA) ($n = 6$); and group IV, animals treated with B[a]P/APAP ($n = 12$). Mice body weight was measured daily. The experimental groups did not exhibit significant differences in body weight.

First, 50 mg/kg B[a]P or sesame oil (vehicle/control) was intraperitoneally (IP) administered to mice for three consecutive days. Twenty-four hours after B[a]P administration, mice were treated with 200 mg/kg APAP or saline (vehicle/control) by a single intraperitoneal injection (IP), followed by euthanization 24 h after co-exposure [26] (Figure 6).

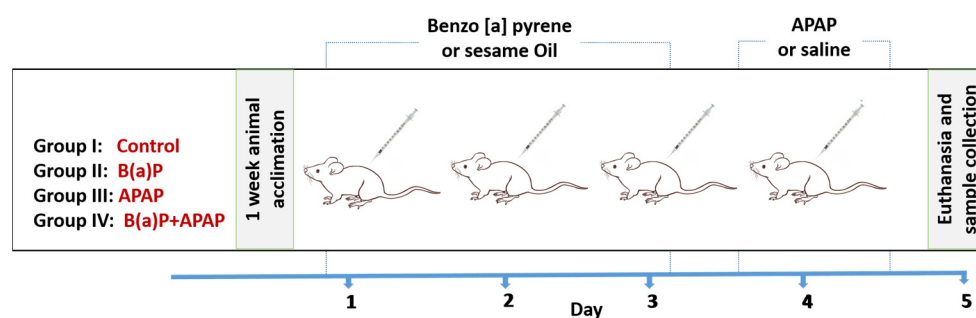


Figure 6. Experimental Design. Animals were given 0 or 50 mg/kg B[a]P for three consecutive days and then exposed to 0 or 200 mg/kg APAP. Mice were euthanized at 24 h after APAP injection.

The doses of 50 mg/kg B[a]P and 200 mg/kg APAP and the number of mice for each experimental group were selected based on a pilot study, which demonstrated that mice treated with this dosage regimen did not exhibit elevations in serum ALT activity (assessed separately for each group) and considering the risk of loss of experimental units from the co-exposed group. IP administration was chosen to ensure the absorption of APAP and B(a)P from the peritoneal cavity by the portal system. The entire experiment was repeated with similar results.

4.3. Sample Collection

After treatment, mice were euthanized by exsanguination under sodium pentobarbital anesthesia administered by IP injection at a dose of 60 mg/kg [86]. Whole blood, collected via the portal vein, was centrifuged at $2000 \times g$ for 15 min at 4 °C. Serum was stored at -80 °C for further analysis. A tissue section of the liver was immediately stored in RNALater® (Qiagen, Germantown, MD, USA) for gene-expression analysis, and another portion was collected in tubes with 10% buffered formalin for histopathological analysis.

4.4. Enzyme Analysis

Serum transaminase activities were measured according to the International Federation of Clinical Chemistry (IFCC) reference method for alanine and aspartate aminotransferase, using commercially available kits (Biosystems S.A., Barcelona, Spain). Test reactions were conducted at 37 °C, with absorbance monitored at 340 nm using a semi-automatic BTS 350 analyzer (Biosystems S.A., Barcelona, Spain).

4.5. Gene Expression Assays

Hepatic RNA was isolated using the RNeasy[®] Mini Kit (Qiagen, Germantown, MD, USA) following the manufacturer's instructions. RNA concentration and purity were determined using a Thermo Scientific Nanodrop 2000 spectrophotometer (Thermo Fisher Scientific, Wilmington, MA, USA). RNA was quantified by spectrophotometry (A260), purity was assessed by the A260/A280 ratio, and integrity was checked by visual inspection on an agarose gel after an electrophoresis run. RNA aliquots were stored at −80 °C for later use.

Extracted RNA (2 µg) was used as a template to synthesize cDNA utilizing a High-Capacity RNA-to-cDNA[™] Kit (Applied Biosystems, Foster City, CA, USA). The cDNA was used as a template in a total volume of 20 µL, containing 10 pmol each of forward and reverse gene-specific primers. The amplification was carried out considering the appropriate annealing temperature for each pair of specific primers for the genes of interest. The Real-Time PCR reaction was performed on a StepOne[®] Real-Time PCR System (Applied Biosystems, Foster City, CA, USA), using the PowerUp[™] SYBR[®] Green Master Mix kit (Applied Biosystems, Foster City, CA, USA).

Eleven genes coding for proteins involved in different biochemical pathways were analyzed, including markers of xenobiotic metabolism, inflammation, apoptosis, oxidative stress, and lipid metabolism. Accession numbers and primer sequences for the target genes are provided in Table S1. Changes in gene expression were determined using the relative standard curve method [87,88]. The fold-change of the target gene expression is presented as the n-fold difference relative to the control group. β-Actin and Rps29 were employed as housekeeping genes.

4.6. Pathological Examination

Liver tissue sections were treated with 10% phosphate-buffered neutral formalin, dehydrated using a graded ethanol series (25–100%), and then embedded in paraffin. The tissue blocks were cut into 5 µm thick slices, deparaffinized with xylene and ethanol, and then stained with hematoxylin and eosin (H&E) for the examination of histopathological changes [86]. Images of different tissue sections were captured using a Nikon ECLIPSE E-100 microscope, coded, and examined in a blinded manner to avoid any type of bias.

The following parameters were examined in liver tissue: ballooning, steatosis, portal inflammation, lobular inflammation, and necrosis. For semi-quantitative effects, each histopathological finding was scored as follows: a score of 0 indicates severity absent or rare; 1, mild; 2, moderate; and 3, marked. Total scores for hepatic histopathology lesions in each mouse were calculated by the sum of scores from each of the parameters found. A minimum pathology was associated with a mouse liver score less than 5, moderate pathology if the total score was 5–10, and marked pathology if it was 10–15 [89,90].

4.7. Statistical Analysis

Results are expressed as the mean ± standard error of the mean (SEM). The normality and homogeneity of variance were verified using the Shapiro–Wilk and Bartlett tests, respectively. Differences between the means of the groups were evaluated by ANOVA, followed by Dunnett's post hoc test. In the absence of normality, the Kruskal–Wallis nonparametric test for independent variables followed by Dunn's post hoc test was used.

Spearman correlation analysis was employed to explore associations between histopathological scores, serum transaminase activities, and fold change of gene expression.

GraphPad Prism version 8.0.0 for Windows (San Diego, CA, USA) was utilized for statistical purposes, and a p -value < 0.05 was considered statistically significant.

5. Conclusions

The present study demonstrates that prior exposure to benzo[a]pyrene increases susceptibility to APAP-induced liver injury during treatment at non-hepatotoxic doses in mice. This susceptibility is attributed to changes in gene expression related to cellular metabolism, redox balance, and regulation of cell proliferation, leading to histopathological alterations in the liver, including ballooning injury, steatosis, inflammation, and necrosis (Figure 5). Consequently, therapeutic doses of APAP may result in liver injury in individuals exposed to B[a]P. Further studies are warranted to elucidate exposome-related factors contributing to acetaminophen-induced liver injury.

Supplementary Materials: The following supporting information can be downloaded at: <https://www.mdpi.com/article/10.3390/scipharm92020030/s1>, Table S1: Primer sequences for gene expression analysis; Figure S1: Body weight of the experimental groups; Figure S2: Relative gene expression in liver of ICR mice co-exposed to B[a]P/APAP; Table S2: Relative gene expression values for experimental groups. Figure S3. Effects of B[a]P/APAP on hepatic morphology and transaminase levels on ICR mice.

Author Contributions: Y.M.-P. carried out conceptualization, methodology, formal analysis, investigation, resources, data curation, writing—original draft preparation, and visualization; J.O.-V. was responsible for writing—review and editing, supervision, project administration, and funding acquisition. All authors have read and agreed to the published version of the manuscript.

Funding: The authors are thankful for the support from the University of Cartagena (Plan to Support Research Groups and Doctoral Programs (2020–2023)) and MinCiencias (Doctoral formation, 647/2014).

Institutional Review Board Statement: The animal study protocol was approved by the Ethics Committee of approved by the Ethics Committee on Scientific Research at the University of Cartagena (Minute No. 106 of 15 March 2018).

Informed Consent Statement: Not applicable.

Data Availability Statement: Data are contained within the article and Supplementary Materials.

Conflicts of Interest: The authors declare no conflicts of interest.

References

1. Gloor, Y.; Schwartz, D.; Samer, C.F. Old problem, new solutions: Biomarker discovery for acetaminophen liver toxicity. *Expert Opin. Drug Metab. Toxicol.* **2019**, *15*, 659–669. [[CrossRef](#)] [[PubMed](#)]
2. Ramachandran, A.; Jaeschke, H. Acetaminophen Hepatotoxicity. *Semin Liver Dis.* **2019**, *39*, 221–234. [[CrossRef](#)] [[PubMed](#)]
3. WHO Web Annex A. World Health Organization Model List of Essential Medicines–23rd List, 2023. In *The Selection and Use of Essential Medicines 2023: Executive Summary of the Report of the 24th WHO Expert Committee on the Selection and Use of Essential Medicines, 24–28 April 2023*; World Health Organization: Geneva, Switzerland, 2023.
4. Bacle, A.; Pronier, C.; Gilardi, H.; Polard, E.; Potin, S.; Scailteux, L.-M. Hepatotoxicity risk factors and acetaminophen dose adjustment, do prescribers give this issue adequate consideration? A French university hospital study. *Eur. J. Clin. Pharmacol.* **2019**, *75*, 1143–1151. [[CrossRef](#)] [[PubMed](#)]
5. Achterbergh, R.; Lammers, L.A.; Kuijsten, L.; Klümpen, H.J.; Mathôt, R.A.A.; Romijn, J.A. Effects of nutritional status on acetaminophen measurement and exposure. *Clin. Toxicol.* **2019**, *57*, 42–49. [[CrossRef](#)] [[PubMed](#)]
6. Zillen, D.; Movig, K.L.L.; Kant, G.; Masselink, J.B.; Mian, P. Impact of malnourishment on the pharmacokinetics of acetaminophen and susceptibility to acetaminophen hepatotoxicity. *Clin. Case Rep.* **2021**, *9*, e04611. [[CrossRef](#)] [[PubMed](#)]
7. Crippin, J.S. Acetaminophen hepatotoxicity: Potentiation by isoniazid. *Am. J. Gastroenterol.* **1993**, *88*, 590–592. [[PubMed](#)]
8. Ging, P.; Mikulich, O.; O'Reilly, K.M. Unexpected paracetamol (acetaminophen) hepatotoxicity at standard dosage in two older patients: Time to rethink 1 g four times daily? *Age Ageing* **2016**, *45*, 566–567. [[CrossRef](#)] [[PubMed](#)]
9. Monte, A.A.; Arriaga Mackenzie, I.; Pattee, J.; Kaiser, S.; Willems, E.; Rumack, B.; Reynolds, K.M.; Dart, R.C.; Heard, K.J. Genetic variants associated with ALT elevation from therapeutic acetaminophen. *Clin. Toxicol.* **2022**, *60*, 1198–1204. [[CrossRef](#)] [[PubMed](#)]
10. Schmidt, L.E.; Dalhoff, K. The impact of current tobacco use on the outcome of paracetamol poisoning. *Aliment. Pharmacol. Ther.* **2003**, *18*, 979–985. [[CrossRef](#)]

11. Cai, X.; Cai, H.; Wang, J.; Yang, Q.; Guan, J.; Deng, J.; Chen, Z. Molecular pathogenesis of acetaminophen-induced liver injury and its treatment options. *J. Zhejiang Univ. Sci. B* **2022**, *23*, 265–285. [[CrossRef](#)]
12. McGill, M.R.; Jaeschke, H. Metabolism and disposition of acetaminophen: Recent advances in relation to hepatotoxicity and diagnosis. *Pharm Res.* **2013**, *30*, 2174–2187. [[CrossRef](#)] [[PubMed](#)]
13. Lee, W.M. Acetaminophen Toxicity: A History of Serendipity and Unintended Consequences. *Clin. Liver Dis.* **2020**, *16*, 34–44. [[CrossRef](#)] [[PubMed](#)]
14. Agrawal, S.; Khazaeni, B. Acetaminophen Toxicity. Available online: <https://www.ncbi.nlm.nih.gov/books/NBK441917/> (accessed on 9 January 2023).
15. Lee, W.M. Acetaminophen (APAP) hepatotoxicity—Isn't it time for APAP to go away? *J Hepatol.* **2017**, *67*, 1324–1331. [[CrossRef](#)] [[PubMed](#)]
16. Park, B.K.; Dear, J.W.; Antoine, D.J. Paracetamol (acetaminophen) poisoning. *BMJ Clin. Evid.* **2015**, *2015*, 2101. [[PubMed](#)]
17. Hinson, J.A.; Roberts, D.W.; James, L.P. Mechanisms of acetaminophen-induced liver necrosis. *Handb. Exp. Pharmacol.* **2010**, *196*, 369–405. [[CrossRef](#)] [[PubMed](#)]
18. Luo, G.; Huang, L.; Zhang, Z. The molecular mechanisms of acetaminophen-induced hepatotoxicity and its potential therapeutic targets. *Exp. Biol. Med.* **2023**, *248*, 412–424. [[CrossRef](#)] [[PubMed](#)]
19. Laine, J.E.; Auriola, S.; Pasanen, M.; Juvonen, R.O. Acetaminophen bioactivation by human cytochrome P450 enzymes and animal microsomes. *Xenobiotica* **2009**, *39*, 11–21. [[CrossRef](#)] [[PubMed](#)]
20. Klopčič, I.; Poberžnik, M.; Mavri, J.; Dolenc, M.S. A quantum chemical study of the reactivity of acetaminophen (paracetamol) toxic metabolite N-acetyl-p-benzoquinone imine with deoxyguanosine and glutathione. *Chem. Biol. Interact.* **2015**, *242*, 407–414. [[CrossRef](#)] [[PubMed](#)]
21. Du, K.; Ramachandran, A.; Jaeschke, H. Oxidative stress during acetaminophen hepatotoxicity: Sources, pathophysiological role and therapeutic potential. *Redox Biol.* **2016**, *10*, 148–156. [[CrossRef](#)]
22. Ramachandran, A.; Jaeschke, H. Oxidant Stress and Acetaminophen Hepatotoxicity: Mechanism-Based Drug Development. *Antioxid. Redox Signal.* **2021**, *35*, 718–733. [[CrossRef](#)]
23. Inkielewicz-Stępnia, I.; Knap, N. Effect of exposure to fluoride and acetaminophen on oxidative/nitrosative status of liver and kidney in male and female rats. *Pharmacol. Rep.* **2012**, *64*, 902–911. [[CrossRef](#)] [[PubMed](#)]
24. Pristner, M.; Warth, B. Drug–Exposome Interactions: The Next Frontier in Precision Medicine. *Trends Pharmacol. Sci.* **2020**, *41*, 994–1005. [[CrossRef](#)] [[PubMed](#)]
25. Aibo, D.I.; Birmingham, N.P.; Lewandowski, R.; Maddox, J.F.; Roth, R.A.; Ganey, P.E.; Wagner, J.G.; Harkema, J.R. Acute exposure to ozone exacerbates acetaminophen-induced liver injury in mice. *Toxicol. Sci.* **2010**, *115*, 267–285. [[CrossRef](#)] [[PubMed](#)]
26. Gardner, C.R.; Mishin, V.; Laskin, J.D.; Laskin, D.L. Exacerbation of acetaminophen hepatotoxicity by the anthelmintic drug fenbendazole. *Toxicol. Sci.* **2012**, *125*, 607–612. [[CrossRef](#)] [[PubMed](#)]
27. Liu, X.; Chen, C.; Zhang, X. Drug–drug interaction of acetaminophen and roxithromycin with the cocktail of cytochrome P450 and hepatotoxicity in rats. *Int. J. Med. Sci.* **2020**, *17*, 414–421. [[CrossRef](#)]
28. Ramachandran, A.; Lebofsky, M.; Yan, H.M.; Weinman, S.A.; Jaeschke, H. Hepatitis C virus structural proteins can exacerbate or ameliorate acetaminophen-induced liver injury in mice. *Arch. Toxicol.* **2015**, *89*, 773–783. [[CrossRef](#)] [[PubMed](#)]
29. Manimaran, A.; Sarkar, S.N.; Sankar, P. Repeated preexposure or coexposure to arsenic differentially alters acetaminophen-induced oxidative stress in rat kidney. *Environ. Toxicol.* **2011**, *26*, 250–259. [[CrossRef](#)] [[PubMed](#)]
30. Deng, C.; Dang, F.; Gao, J.; Zhao, H.; Qi, S.; Gao, M. Acute benzo[a]pyrene treatment causes different antioxidant response and DNA damage in liver, lung, brain, stomach and kidney. *Heliyon* **2018**, *4*, e00898. [[CrossRef](#)] [[PubMed](#)]
31. Guo, B.; Feng, D.; Xu, Z.; Qi, P.; Yan, X. Acute benzo[a]pyrene exposure induced oxidative stress, neurotoxicity and epigenetic change in blood clam *Tegillarca granosa*. *Sci. Rep.* **2021**, *11*, 18744. [[CrossRef](#)]
32. Salamat, N.; Derakhshesh, N. Oxidative stress in liver cell culture from mullet, *Liza klunzingeri*, induced by short-term exposure to benzo[a]pyrene and nonylphenol. *Fish Physiol. Biochem.* **2020**, *46*, 1183–1197. [[CrossRef](#)]
33. ATSDR Agency for Toxic Substances and Disease Registry (ATSDR). ATSDR's Substance Priority List. Available online: <https://www.atsdr.cdc.gov/SPL/> (accessed on 25 April 2023).
34. Ramesh, A.; Harris, K.J.; Archibong, A.E. Chapter 40—Reproductive Toxicity of Polycyclic Aromatic Hydrocarbons. In *Reproductive and Developmental Toxicology*, 2nd ed.; Gupta, R.C., Ed.; Academic Press: Cambridge, MA, USA, 2017; pp. 745–763.
35. Bukowska, B.; Mokra, K. Benzo[a]pyrene—Environmental Occurrence, Human Exposure, and Mechanisms of Toxicity. *Int. J. Mol. Sci.* **2022**, *23*, 6348. [[CrossRef](#)] [[PubMed](#)]
36. Kim, N.Y.; Loganathan, B.G.; Kim, G.B. Determination and comparison of freely dissolved PAHs using different types of passive samplers in freshwater. *Sci. Total Environ.* **2023**, *892*, 164802. [[CrossRef](#)] [[PubMed](#)]
37. Belykh, L.I.; Maksimova, M.A. Benzo(a)pyrene in the atmosphere and its carcinogenic risks to the health of the population of Irkutsk region cities. *IOP Conf. Ser. Earth Environ. Sci.* **2022**, *1061*, 012003. [[CrossRef](#)]
38. EPA, U.S. *IRIS Toxicological Review of Benzo[A]Pyrene (Final Report)*; U.S. Environmental Protection Agency: Washington, DC, USA, 2017; EPA/635/R-17/003F, 2017.
39. IARC. Working Group on the Evaluation of Carcinogenic Risk to Humans. In *Chemical Agents and Related Occupations*; International Agency for Research on Cancer: Lyon, France, 2012; IARC Monographs on the Evaluation of Carcinogenic Risks to Humans, No. 100F.

40. Jorge, B.C.; Reis, A.C.C.; Stein, J.; Balin, P.D.S.; Sterde, É.T.; Barbosa, M.G.; de Aquino, A.M.; Kassuya, C.A.L.; Arena, A.C. Parental exposure to benzo(a)pyrene in the peripubertal period impacts reproductive aspects of the F1 generation in rats. *Reprod. Toxicol.* **2021**, *100*, 126–136. [[CrossRef](#)] [[PubMed](#)]
41. Sadikovic, B.; Andrews, J.; Carter, D.; Robinson, J.; Rodenhiser, D.I. Genome-wide H3K9 histone acetylation profiles are altered in benzopyrene-treated MCF7 breast cancer cells. *J. Biol. Chem.* **2008**, *283*, 4051–4060. [[CrossRef](#)] [[PubMed](#)]
42. Gao, M.; Li, Y.; Sun, Y.; Shah, W.; Yang, S.; Wang, Y.; Long, J. Benzo[a]pyrene exposure increases toxic biomarkers and morphological disorders in mouse cervix. *Basic. Clin. Pharmacol. Toxicol.* **2011**, *109*, 398–406. [[CrossRef](#)] [[PubMed](#)]
43. Bukowska, B.; Duchnowicz, P. Molecular Mechanisms of Action of Selected Substances Involved in the Reduction of Benzo[a]pyrene-Induced Oxidative Stress. *Molecules* **2022**, *27*, 1379. [[CrossRef](#)] [[PubMed](#)]
44. Hodek, P.; Koblihová, J.; Kizek, R.; Frei, E.; Arlt, V.M.; Stiborová, M. The relationship between DNA adduct formation by benzo[a]pyrene and expression of its activation enzyme cytochrome P450 1A1 in rat. *Environ. Toxicol. Pharmacol.* **2013**, *36*, 989–996. [[CrossRef](#)] [[PubMed](#)]
45. Moorthy, B.; Chu, C.; Carlin, D.J. Polycyclic aromatic hydrocarbons: From metabolism to lung cancer. *Toxicol. Sci. Off. J. Soc. Toxicol.* **2015**, *145*, 5–15. [[CrossRef](#)] [[PubMed](#)]
46. Piberger, A.L.; Krüger, C.T.; Strauch, B.M.; Schneider, B.; Hartwig, A. BPDE-induced genotoxicity: Relationship between DNA adducts, mutagenicity in the in vitro PIG-A assay, and the transcriptional response to DNA damage in TK6 cells. *Arch. Toxicol.* **2018**, *92*, 541–551. [[CrossRef](#)]
47. Palackal, N.T.; Burczynski, M.E.; Harvey, R.G.; Penning, T.M. The Ubiquitous Aldehyde Reductase (AKR1A1) Oxidizes Proximate Carcinogen trans-Dihydrodiols to o-Quinones: Potential Role in Polycyclic Aromatic Hydrocarbon Activation. *Biochemistry* **2001**, *40*, 10901–10910. [[CrossRef](#)]
48. Huang, M.; Blair, I.A.; Penning, T.M. Identification of Stable Benzo[a]pyrene-7,8-dione-DNA Adducts in Human Lung Cells. *Chem. Res. Toxicol.* **2013**, *26*, 685–692. [[CrossRef](#)] [[PubMed](#)]
49. Licata, A.; Minissale, M.G.; Stankevičiūtė, S.; Sanabria-Cabrera, J.; Lucena, M.I.; Andrade, R.J.; Almasio, P.L. N-Acetylcysteine for Preventing Acetaminophen-Induced Liver Injury: A Comprehensive Review. *Front. Pharmacol.* **2022**, *13*, 828565. [[CrossRef](#)] [[PubMed](#)]
50. Santoh, M.; Sanoh, S.; Takagi, M.; Ejiri, Y.; Kotake, Y.; Ohta, S. Acetaminophen induces accumulation of functional rat CYP3A via polyubiquitination dysfunction. *Sci. Rep.* **2016**, *6*, 21373. [[CrossRef](#)] [[PubMed](#)]
51. Huang, Y.-J.; Chen, P.; Lee, C.-Y.; Yang, S.-Y.; Lin, M.-T.; Lee, H.-S.; Wu, Y.-M. Protection against acetaminophen-induced acute liver failure by omentum adipose tissue derived stem cells through the mediation of Nrf2 and cytochrome P450 expression. *J. Biomed. Sci.* **2016**, *23*, 5. [[CrossRef](#)] [[PubMed](#)]
52. Schuran, F.A.; Lommetz, C.; Steudter, A.; Ghallab, A.; Wieschendorf, B.; Schwinge, D.; Zuehlke, S.; Reinders, J.; Heeren, J.; Lohse, A.W.; et al. Aryl Hydrocarbon Receptor Activity in Hepatocytes Sensitizes to Hyperacute Acetaminophen-Induced Hepatotoxicity in Mice. *Cell Mol. Gastroenterol. Hepatol.* **2020**, *11*, 371–388. [[CrossRef](#)] [[PubMed](#)]
53. Trefts, E.; Gannon, M.; Wasserman, D.H. The liver. *Curr. Biol.* **2017**, *27*, R1147–R1151. [[CrossRef](#)] [[PubMed](#)]
54. Knuckles, M.E.; Inyang, F.; Ramesh, A. Acute and Subchronic Oral Toxicities of Benzo[a]pyrene in F-344 Rats. *Toxicol. Sci.* **2001**, *61*, 382–388. [[CrossRef](#)] [[PubMed](#)]
55. Yoshida, M.; Umemura, T.; Kojima, H.; Inoue, K.; Takahashi, M.; Uramaru, N.; Kitamura, S.; Abe, K.; Tohkin, M.; Ozawa, S.; et al. Basic principles of interpretation of hepatocellular hypertrophy in risk assessment in Japan. *Shokuhin Eiseigaku Zasshi* **2015**, *56*, 42–48. [[CrossRef](#)]
56. Šulc, M.; Indra, R.; Moserová, M.; Schmeiser, H.H.; Frei, E.; Arlt, V.M.; Stiborová, M. The impact of individual cytochrome P450 enzymes on oxidative metabolism of benzo[a]pyrene in human livers. *Environ. Mol. Mutagen.* **2016**, *57*, 229–235. [[CrossRef](#)]
57. Mazaleuskaya, L.L.; Sangkuhl, K.; Thorn, C.F.; FitzGerald, G.A.; Altman, R.B.; Klein, T.E. PharmGKB summary: Pathways of acetaminophen metabolism at the therapeutic versus toxic doses. *Pharmacogenet. Genom.* **2015**, *25*, 416–426. [[CrossRef](#)] [[PubMed](#)]
58. Asweto, C.O.; Wu, J.; Hu, H.; Feng, L.; Yang, X.; Duan, J.; Sun, Z. Combined Effect of Silica Nanoparticles and Benzo[a]pyrene on Cell Cycle Arrest Induction and Apoptosis in Human Umbilical Vein Endothelial Cells. *Int. J. Environ. Res. Public Health* **2017**, *14*, 289. [[CrossRef](#)]
59. Youbin, Q.; Chengzhi, C.; Yan, T.; Xuejun, J.; Chongying, Q.; Bin, P.; Baijie, T. The synergistic effect of benzo[a]pyrene and lead on learning and memory of mice. *Toxicol. Ind. Health* **2013**, *29*, 387–395. [[CrossRef](#)] [[PubMed](#)]
60. Uppstad, H.; Øvrebø, S.; Haugen, A.; Mollerup, S. Importance of CYP1A1 and CYP1B1 in bioactivation of benzo[a]pyrene in human lung cell lines. *Toxicol. Lett.* **2010**, *192*, 221–228. [[CrossRef](#)] [[PubMed](#)]
61. Stevens, E.A.; Mezrich, J.D.; Bradfield, C.A. The aryl hydrocarbon receptor: A perspective on potential roles in the immune system. *Immunology* **2009**, *127*, 299–311. [[CrossRef](#)] [[PubMed](#)]
62. Vázquez-Gómez, G.; Rubio-Lightbourn, J.; Espinosa-Aguirre, J.J. Mecanismos de acción del receptor de hidrocarburos de arilos en el metabolismo del benzo[a]pireno y el desarrollo de tumores. *TIP. Rev. Espec. Cienc. Químico-Biológicas* **2016**, *19*. [[CrossRef](#)]
63. Mimura, J.; Fujii-Kuriyama, Y. Functional role of AhR in the expression of toxic effects by TCDD. *Biochim. Biophys. Acta BBA Gen. Subj.* **2003**, *1619*, 263–268. [[CrossRef](#)]
64. Bucher, S.; Tête, A.; Podechard, N.; Liamin, M.; Le Guillou, D.; Chevanne, M.; Coulouarn, C.; Imran, M.; Gallais, I.; Fernier, M.; et al. Co-exposure to benzo[a]pyrene and ethanol induces a pathological progression of liver steatosis in vitro and in vivo. *Sci. Rep.* **2018**, *8*, 5963. [[CrossRef](#)]

65. Morel, Y.; de Waziers, I.; Barouki, R. A repressive cross-regulation between catalytic and promoter activities of the CYP1A1 and CYP2E1 genes: Role of H(2)O(2). *Mol. Pharmacol.* **2000**, *57*, 1158–1164.
66. Morel, Y.; Mermoud, N.; Barouki, R. An autoregulatory loop controlling CYP1A1 gene expression: Role of H(2)O(2) and NFI. *Mol. Cell Biol.* **1999**, *19*, 6825–6832. [[CrossRef](#)]
67. Thummel, K.E.; Lee, C.A.; Kunze, K.L.; Nelson, S.D.; Slattery, J.T. Oxidation of acetaminophen to N-acetyl-p-aminobenzoquinone imine by Human CYP3A4. *Biochem. Pharmacol.* **1993**, *45*, 1563–1569. [[CrossRef](#)]
68. Yang, Y.; Wong, S.E.; Lightstone, F.C. Understanding a substrate's product regioselectivity in a family of enzymes: A case study of acetaminophen binding in cytochrome P450s. *PLoS ONE* **2014**, *9*, e87058. [[CrossRef](#)] [[PubMed](#)]
69. Zaher, H.; Buters, J.T.; Ward, J.M.; Bruno, M.K.; Lucas, A.M.; Stern, S.T.; Cohen, S.D.; Gonzalez, F.J. Protection against acetaminophen toxicity in CYP1A2 and CYP2E1 double-null mice. *Toxicol. Appl. Pharmacol.* **1998**, *152*, 193–199. [[CrossRef](#)]
70. Lee, S.S.T.; Buters, J.T.M.; Pineau, T.; Fernandez-Salguero, P.; Gonzalez, F.J. Role of CYP2E1 in the Hepatotoxicity of Acetaminophen. *J. Biol. Chem.* **1996**, *271*, 12063–12067. [[CrossRef](#)] [[PubMed](#)]
71. McGill, M.R.; Hinson, J.A. The development and hepatotoxicity of acetaminophen: Reviewing over a century of progress. *Drug Metab. Rev.* **2020**, *52*, 472–500. [[CrossRef](#)]
72. Muhammad-Azam, F.; Nur-Fazila, S.H.; Ain-Fatin, R.; Mustapha Noordin, M.; Yimer, N. Histopathological changes of acetaminophen-induced liver injury and subsequent liver regeneration in BALB/C and ICR mice. *Vet. World* **2019**, *12*, 1682–1688. [[CrossRef](#)]
73. Sánchez-Rodríguez, R.; Torres-Mena, J.E.; del Pozo Yauner, L.; Pérez-Carreón, J.I. Biomarkers of the Antioxidant Response: A Focus on Liver Carcinogenesis. In *Biomarkers in Liver Disease*; Patel, V.B., Preedy, V.R., Eds.; Springer: Dordrecht, The Netherlands, 2017; pp. 785–808.
74. Milani, P.; Gagliardi, S.; Cova, E.; Cereda, C. SOD1 Transcriptional and Posttranscriptional Regulation and Its Potential Implications in ALS. *Neurol. Res. Int.* **2011**, *2011*, 458427. [[CrossRef](#)] [[PubMed](#)]
75. Pan, J.; Zhou, W.; Xu, R.; Xing, L.; Ji, G.; Dang, Y. Natural PPARs agonists for the treatment of nonalcoholic fatty liver disease. *Biomed. Pharmacother.* **2022**, *151*, 113127. [[CrossRef](#)]
76. Janani, C.; Ranjitha Kumari, B.D. PPAR gamma gene—A review. *Diabetes Metab Syndr.* **2015**, *9*, 46–50. [[CrossRef](#)]
77. Lou, W.; Zhang, M.D.; Chen, Q.; Bai, T.Y.; Hu, Y.X.; Gao, F.; Li, J.; Lv, X.L.; Zhang, Q.; Chang, F.H. Molecular mechanism of benzo[a]pyrene regulating lipid metabolism via aryl hydrocarbon receptor. *Lipids Health Dis.* **2022**, *21*, 13. [[CrossRef](#)]
78. Videla, L.A.; Pettinelli, P. Misregulation of PPAR Functioning and Its Pathogenic Consequences Associated with Nonalcoholic Fatty Liver Disease in Human Obesity. *PPAR Res.* **2012**, *2012*, 107434. [[CrossRef](#)] [[PubMed](#)]
79. Begriche, K.; Penhoat, C.; Bernabeu-Gentey, P.; Massart, J.; Fromenty, B. Acetaminophen-Induced Hepatotoxicity in Obesity and Nonalcoholic Fatty Liver Disease: A Critical Review. *Livers* **2023**, *3*, 33–53. [[CrossRef](#)] [[PubMed](#)]
80. García-Román, R.; Francés, R. Acetaminophen-Induced Liver Damage in Hepatic Steatosis. *Clin. Pharmacol. Ther.* **2020**, *107*, 1068–1081. [[CrossRef](#)] [[PubMed](#)]
81. Kučera, O.; Al-Dury, S.; Lotková, H.; Roušar, T.; Rychtmoc, D.; Červinková, Z. Steatotic rat hepatocytes in primary culture are more susceptible to the acute toxic effect of acetaminophen. *Physiol. Res.* **2012**, *61*, S93–S101. [[CrossRef](#)] [[PubMed](#)]
82. Zhao, B.; Xin, Z. The Role of PPARs in Breast Cancer. *Cells* **2022**, *12*, 130. [[CrossRef](#)] [[PubMed](#)]
83. Rathore, K.; Cekanova, M. Effects of environmental carcinogen benzo(a)pyrene on canine adipose-derived mesenchymal stem cells. *Res. Veter. Sci.* **2015**, *103*, 34–43. [[CrossRef](#)] [[PubMed](#)]
84. Tsubouchi, Y.; Sano, H.; Kawahito, Y.; Mukai, S.; Yamada, R.; Kohno, M.; Inoue, K.; Hla, T.; Kondo, M. Inhibition of human lung cancer cell growth by the peroxisome proliferator-activated receptor-gamma agonists through induction of apoptosis. *Biochem. Biophys. Res. Commun.* **2000**, *270*, 400–405. [[CrossRef](#)] [[PubMed](#)]
85. Kato, Y.; Ying, H.; Zhao, L.; Furuya, F.; Araki, O.; Willingham, M.C.; Cheng, S.Y. PPARgamma insufficiency promotes follicular thyroid carcinogenesis via activation of the nuclear factor-kappaB signaling pathway. *Oncogene* **2006**, *25*, 2736–2747. [[CrossRef](#)] [[PubMed](#)]
86. Caballero-Gallardo, K.; Olivero-Verbel, J. Mice housed on coal dust-contaminated sand: A model to evaluate the impacts of coal mining on health. *Toxicol. Appl.* **2016**, *294*, 11–20. [[CrossRef](#)]
87. Applied-Biosystems. *Guide to Performing Relative Quantitation of Gene Using Real-Time Quantitative PCR*; Applied-Biosystems: Foster City, CA, USA, 2008; Part Number 4371095 Rev B.
88. Nolan, T.; Hands, R.E.; Bustin, S.A. Quantification of mRNA using real-time RT-PCR. *Nat Protoc.* **2006**, *1*, 1559–1582. [[CrossRef](#)]
89. Damiri, B.; Holle, E.; Yu, X.; Baldwin, W.S. Lentiviral-mediated RNAi knockdown yields a novel mouse model for studying Cyp2b function. *Toxicol. Sci.* **2012**, *125*, 368–381. [[CrossRef](#)] [[PubMed](#)]
90. Kleiner, D.E.; Brunt, E.M.; Van Natta, M.; Behling, C.; Contos, M.J.; Cummings, O.W.; Ferrell, L.D.; Liu, Y.C.; Torbenson, M.S.; Unalp-Arida, A.; et al. Design and validation of a histological scoring system for nonalcoholic fatty liver disease. *Hepatology* **2005**, *41*, 1313–1321. [[CrossRef](#)] [[PubMed](#)]

Disclaimer/Publisher's Note: The statements, opinions and data contained in all publications are solely those of the individual author(s) and contributor(s) and not of MDPI and/or the editor(s). MDPI and/or the editor(s) disclaim responsibility for any injury to people or property resulting from any ideas, methods, instructions or products referred to in the content.